NASA Technical Paper 1369

Transient Shutdown Analysis of Low-Temperature Thermal Diodes

Richard J. Williams

MARCH 1979

NASA

NASA Technical Paper 1369

Transient Shutdown Analysis of Low-Temperature Thermal Diodes

Richard J. Williams
Ames Research Center
Moffett Field, California

National Aeronautics
and Space Administration

**Scientific and Technical
Information Office**

1979

TRANSIENT SHUTDOWN ANALYSIS OF LOW-TEMPERATURE THERMAL DIODES

Richard J. Williams*

Ames Research Center

The various thermal diodes available for use in cryogenic systems are described. Two diode types, liquid-trap and liquid-blockage diodes, were considered to be the most attractive, and thermal models were constructed to predict their behavior in the reverse mode.

The diodes, which used spiral artery wicks, were of similar size and throughput and were examined experimentally in a parallel test setup under nominally identical conditions. Their characteristics were ascertained in terms of forward-mode and reverse-mode conductances, shutdown times and energies, and recovery to forward-mode operation with ethane as the working fluid in the temperature range 170 K to 220 K.

Test data compare well with the data obtained with single heat pipe testing. Results show that the liquid-blockage diode is the quicker of the two diodes to shut down from the forward mode and that it transfers less energy to its evaporator during shutdown (8 min and 296 J as opposed to 10 min and 1150 J). However, the liquid-blockage diode has a larger reverse-mode conductance which results in a greater overall evaporator temperature rise.

The selection of the relative size and heat inputs to the condenser/reservoir configuration of the liquid-blockage diode was shown to be an important factor in the operation of the diode if the evaporator is to be protected from a rapid increase in temperature after a reversal. Also included are data that show that the reinitiation of heat-piping action during recovery to forward-mode operation cannot be guaranteed if a limit in cool-down rate of the condenser is exceeded. This limit was found to be 1 K/min for the liquid-trap diode and 2 K/min for the liquid-blockage diode. General guidelines for the choice of a particular diode for an actual application are also given.

Heat pipes are continuing to be developed to meet increasingly difficult requirements of spacecraft thermal control. Although extensive studies of both active and passive variable conductance heat pipes for fine temperature control have been carried out, many applications exist wherein the ability of the heat pipe to conduct heat efficiently in one direction is of primary importance. Such heat pipes are described as thermal diodes (refs. 1, 2). These diodes are attractive for use in the cryogenic temperature range. In the near future a large number of cryogenic payloads are due to be flown. In one proposed application, diode heat pipes are used to extract heat from a low-temperature sensor, such as an infrared detector, and to thermally disconnect the sensor to prevent overheating should the radiator be exposed to a sudden high external heat flux. Using this concept, low-temperature cooling can be provided in low subsolar Earth orbits where radiator cooling was never before considered possible.

Several diode techniques have been identified (ref. 1). These include the use of noncondensable gas, liquid-flow control, and freezing of the working fluid. More recently the concept of employing a foil reed in the vapor space to shut off the diode in the reverse mode has also been suggested. From these diodes, two types of liquid flow control were considered to be the most attractive: the liquid-trap diode and the liquid-blockage diode.

The liquid-trap concept employs a reservoir situated at the normal evaporator end of the pipe which does not communicate with the wick. In normal-mode operation the trap contains no liquid, and the diode performs as a normal heat pipe (cf. fig. 1). During reverse-mode operation the trap becomes the cold end of the pipe and condensation of the working fluid occurs inside the trap. The wick is thus depleted of working fluid and a rapid reduction of transport capability results until all the fluid is condensed in the trap. Throughput is then limited to conduction heat transfer along the wall and wick. When conditions again reverse themselves, the trap becomes the hot end of the pipe and acts as an evaporator until all the liquid is expelled and normal heat pipe action is resumed.

With the liquid-blockage technique the heat pipe is charged with excess fluid. In normal-mode operation this excess fluid collects in a reservoir situated at the condenser end of the pipe (fig. 1). Under reverse-mode operation this excess liquid migrates to the cold

*NRC Resident Research Associate

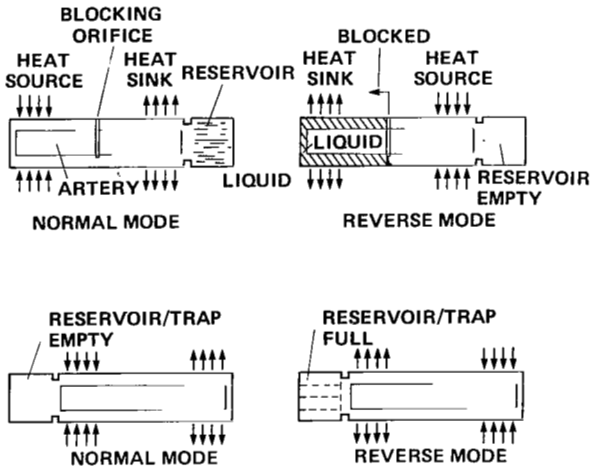

Figure 1.– Liquid-trap and liquid-blockage concepts.

end and there occupies a volume sufficient to block the vapor space of the normal evaporator together with a portion of the transport section. Due to its low thermal conductivity, the liquid very effectively limits the heat transfer in this section of the device. This diode technique is attractive for cryogenic applications where the normal-mode evaporator is relatively short compared with the condenser. This configuration minimizes the excess liquid required for blockage and thus minimizes the reservoir size, whereas with the liquid trap the reservoir must be sized to hold the majority of fluid in the pipe. This results in the trap being larger than the reservoir required for liquid blockage, and thus the liquid blockage diode has a weight advantage over the trap diode. However, an important factor in cryogenic diodes is the pipe pressure under ambient conditions; for constant outside diameter and a given wick, the highest specific volume and therefore the lowest pressure are obtained with the liquid-trap technique.

Thus, there still exists much conjecture and debate about the relative performance characteristics of the two devices. The purpose of this study was, therefore, to examine both mechanisms under identical conditions to ascertain their characteristics in terms of shutdown times and energies, reverse-mode conductance, and recovery to forward-mode operation. It is hoped that the results obtained from this investigation will provide valuable guidelines for designers in the choice of a diode to meet their requirements.

NOMENCLATURE

A	area
C_f	forward-mode conductance
F_T, F_B	Q/MC_P ratios (eqs. (2) and (3))
h	heat-transfer coefficient
k	thermal conductivity
L	length
P	pressure
$\mathring{Q}$	heat input rate
Q	heat input
R	ratio condensation rate in evaporator to condensation rate in trap
r	bubble radius
T	temperature
t	time
V	volume

Subscripts:

c	condenser
DO	dryout
e	evaporator
Ext	external (area)
Int	internal (area)
J	joint
R	reservoir
SD	shutdown
t	trap

DIODE CONSTRUCTION AND TEST SETUP

Both arterial wicks and axial grooves are suitable for the capillary system of a liquid-trap diode. Axial grooves, although more reliable, are inferior in transport capacity to similarly sized arterial wicks; until recently they have only been produced from aluminum (ref. 3) which results in a higher reverse-mode conductance than that of a stainless steel pipe. The liquid-blockage diode, on the other hand, is almost entirely confined to an arterial wicking system. An axial-groove diode incorporating a plug in the evaporator vapor space has been suggested for spacecraft applications. However, the difficulties that would be encountered in a 1-g test situation, such as draining of the upper grooves due to liquid communication between the grooves in the blocked portion, have precluded any development of such a diode.

The artery diode must be designed to insure that the vapor space in the blocked portion is small enough so that the capillary force will support the pressure head of the liquid slug in 1-g ground tests. This is necessary for the vapor space to prime and remain filled in the reverse mode. These small vapor spaces produce large vapor pressure drops in the normal mode of operation and thus restrict the capacity of the heat pipe. To circumvent this limitation, which is particularly severe at low temperatures where the fluids have low capillary-rise characteristics, a new geometry has been developed (ref. 4). An orifice plate is inserted in the heat pipe at the blocking meniscus, the opening of the plate being at the bottom of the pipe as shown in figure 2. The increased vapor flow area gained by the large evaporator vapor space more than compensates for the additional vapor pressure loss introduced by the orifice.

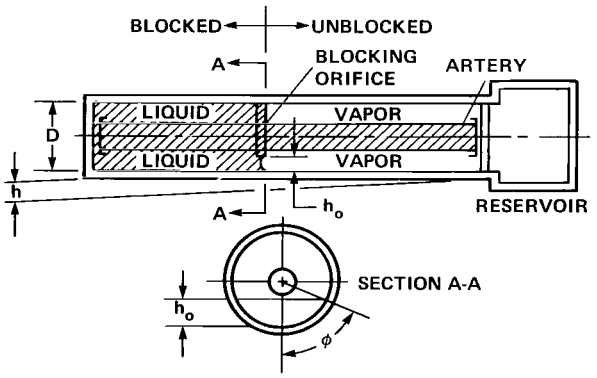

Figure 2.– Blocking orifice – liquid blockage.

To allow performance comparisons, one diode of each type was constructed, each with a spiral artery wick and identical diameter and effective lengths to give comparable forward-mode conductances. The liquid-blockage design includes the aforementioned orifice plate – the liquid-trap heat pipe therefore has a slightly higher throughput, the difference representing the blocking orifice pressure loss.

The fabricated diodes consist of four sections: an evaporator, a transport section, a condenser, and either a liquid trap or liquid reservoir. The wicks were formed by wrapping 250 mesh stainless steel and 0.04-cm-diameter spaces on a mandril (see fig. 3). A transition section at the evaporator end of the liquid-trap diode is integral with a cylindrical reservoir having an inner core of aluminum channel. Similarly, a transition section at the condenser end of the liquid-blockage diode connects a reservoir to the heat pipe. No liquid communication, that is, no capillary connection, was provided between the reservoir and wick of the liquid-trap diode or between the reservoir and wick of the liquid-blockage diode. Liquid communication was achieved between the arteries and the condenser and evaporator walls with three equally spaced scroll-type webs manufactured from 250 mesh stainless steel screen. Circumferential grooves (63/cm) were used in both the evaporator and condenser sections. Detailed design dimensions of the pipes are summarized in table 1.

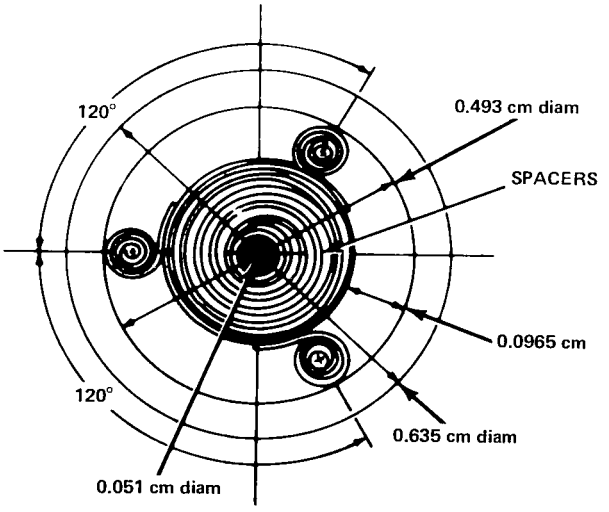

Figure 3.– Wick geometry.

TABLE 1.– HEAT PIPE DESIGN DATA

	Liquid trap	Liquid blockage
Lengths, cm		
Evaporator	10.16	10.16
Transport		
Blocked	0	10.16
Unblocked	28.26	18.10
Condenser	30.48	30.48
Reservoir/trap	15.56	6.03
Effective	48.57	48.57
Diameters, cm		
Pipe, o.d.	.635	.635
Pipe, i.d.	.493	.493
Artery, o.d.	.300	.300
Solid tunnel, o.d.	.051	.051
Reservoir/trap, o.d.	1.588	1.588

Other pertinent design information includes:

Pipes	304 – 1/8 HD stainless steel
Screening	250-mesh 304 stainless steel
Circumferential grooves	63/cm (160/in.)
Reservoir/trap	6061 aluminum laminates 0.239 cm thick with 0.127 cm wide × 0.127 cm deep axial machined grooves. Core machined to 1.448 cm o.d. for press fit into 304 – 1/8 HD stainless steel cylindrical shell

The condensers of both diodes were enclosed in an aluminum block (fig. 4) which mated to a liquid nitrogen sink. Evaporator masses of 0.168 kg were attached to each evaporator to simulate a detector assembly and aluminum masses were also attached to the trap (0.423 kg) and to the liquid-blockage reservoir (0.182 kg). Strip heaters were attached to the evaporators and to the liquid trap to simulate forward-mode heat loads; rod heaters in the condenser block controlled the forward-mode temperature and, together with strip heaters on the liquid reservoir, provided a means for diode reversal. Both the liquid trap and the liquid reservoir were in contact with an LN_2 cooling loop to facilitate a rapid cool-down and a wide range of temperature control.

The locations of the thermocouples used to monitor the local temperature of the heat pipes are shown in figure 4. The rod heaters and a thermocouple embedded in the LN_2 sink were connected to a unit that provides temperature control for the condenser sink. Once assembled, the diode package was wrapped in 30 layers of multilayer insulation (MLI) before being inserted into a vacuum chamber. The MLI density was 30 layers/cm. All testing was performed in the vacuum chamber, which had ambient temperature wells.

TRANSIENT SHUTDOWN MODELS

Liquid Trap

If the liquid-trap diode is shut down directly from the forward mode of operation, there will be a temperature gradient from the evaporator to the condenser. Therefore, immediately after the initiation of shutdown the diode will continue to operate in the forward mode until the condenser temperature is greater than both the evaporator and vapor temperature. The temperature difference between the evaporator and the condenser and the sensible heat stored in the evaporator tend to retard the onset of shutdown. This retardation is linearly dependent on the forward-mode heat throughput. This time delay has not been accounted for in the thermal model to be detailed below.

After the onset of shutdown, that is, with the condenser temperature greater than the evaporator temperature, the heat flow in the diode was reversed. Liquid was evaporated from the condenser and the vapor was condensed in the evaporator and trap. While the fluid that condensed in the trap remained there, the fluid that condensed in the evaporator was wicked back to the condenser to be reevaporated and maintained an adverse heat piping action. The transient shutdown process of the diode therefore depended on the ratio of evaporator condensation rate to trap condensation rate. This ratio was designated R.

A thermal nodal model of the liquid-trap diode system is shown in figure 5.

By lumping together several parameters and neglecting the thermal inertia of the vapor, the condenser can be coupled directly to the evaporator and trap by the overall forward-mode conductance of the pipe. In this manner the simplified model of figure 6 was obtained.

The maximum heat transport capability of the diode was a function of liquid inventory and was

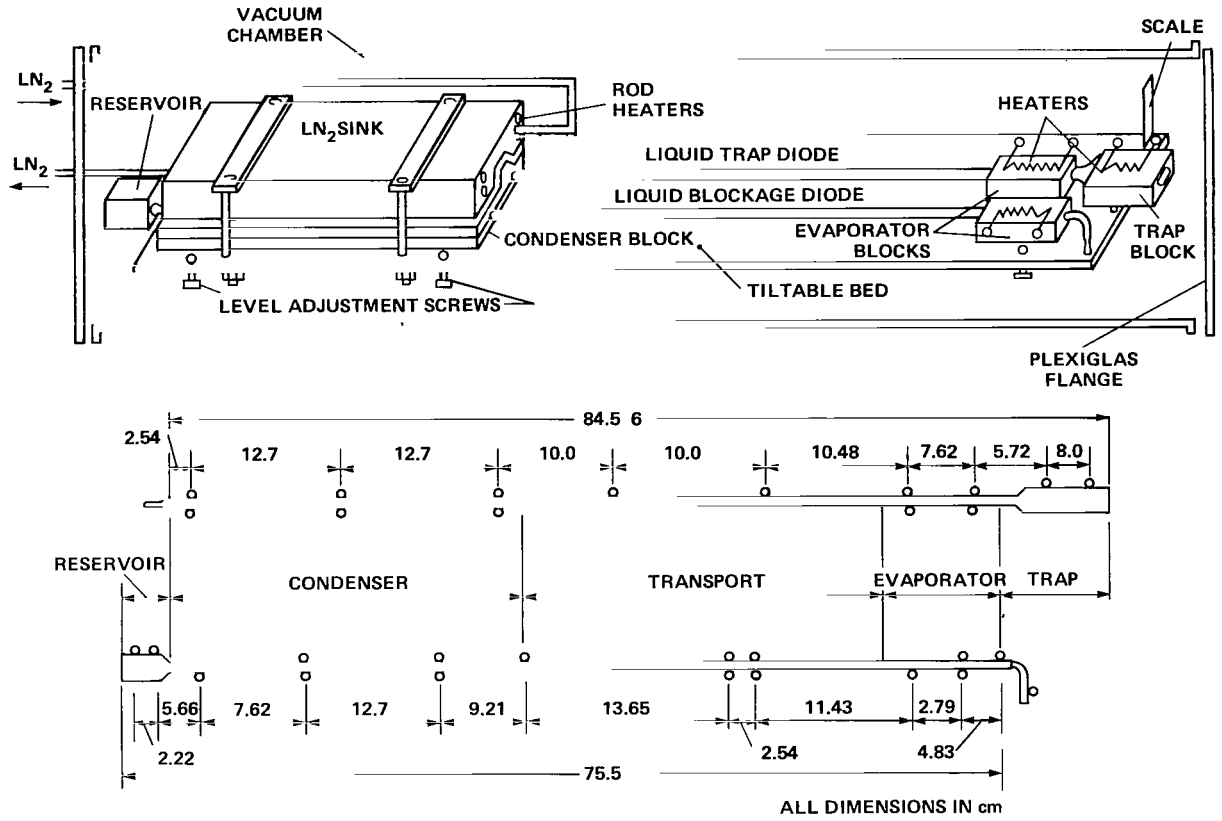

Figure 4.– Experimental apparatus and thermocouple locations.

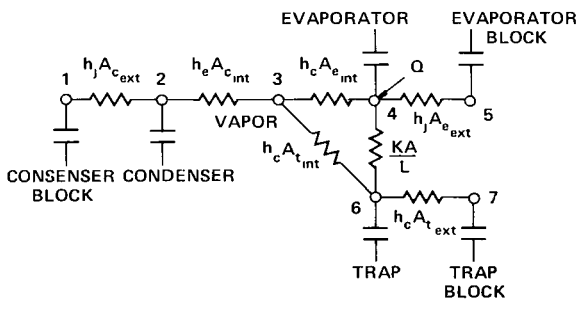

Figure 5.– Thermal nodal model (liquid trap).

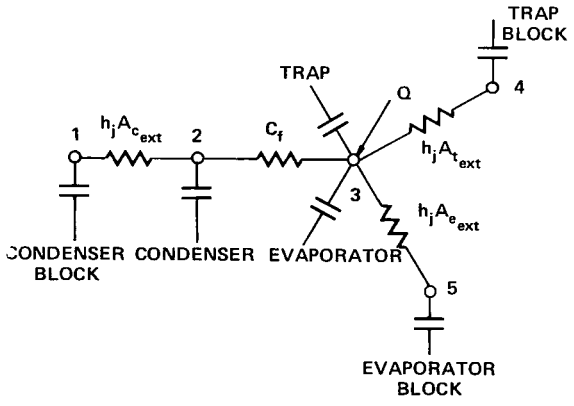

Figure 6.– Simplified model (liquid trap).

independent (within bounds) of temperature. The overall forward-mode conductance also has a unique relationship with fluid inventory, which has been determined experimentally for this diode and is shown in figure 7.

The effective heat-transfer coefficient due to the thermal contact resistance of the joints between the evaporator, condenser, and trap and their respective blocks was taken to be 1.136×10^3 W/m^2 K.

The quantity that describes the ratio of condensation rate in the evaporator (R) cannot be precisely

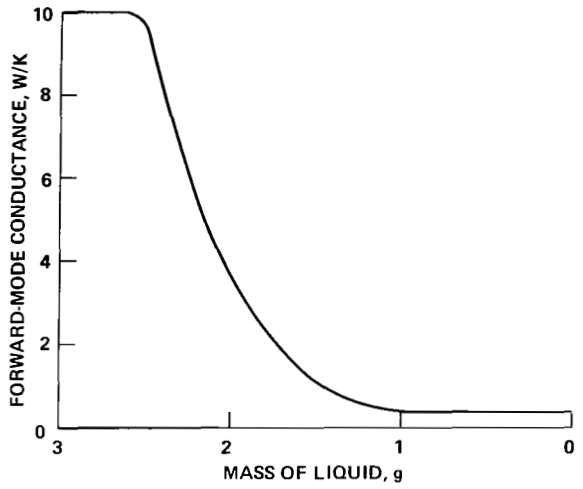

Figure 7.– Forward-mode conductance vs fluid charge.

calculated. Based on the ratio of evaporator-area-to-trap-area the figure becomes approximately 0.1. This implies that 10 times more fluid would be condensed in the trap than in the evaporator, due to its larger area, and would result in a rapid shutdown. However, this is misleading as the vapor flow into the trap is severely restricted because of small channel openings of the trap (0.127 X 0.127 cm). For numerical calculations, an empirically determined figure of R = 0.5 has been used which adequately describes this restriction.

The shutdown model was solved numerically using a thermal analyzer computer program. The transient shutdown power curve is shown in figure 8 for ramp inputs to the condenser block node of 1 K/min and 2 K/min. The figure shows that the throughput peaks at 2.5 min and 9.8 W for the 2 K/min case and at 4 min and 6.2 W for the 1 K/min case. In both cases the throughput reaches a minimum and then increases slowly. This slow increase is due to the finite reverse-mode conductance of the heat pipe wall and wick and the increasing temperature difference between the evaporator and condenser.

By integrating the area under these curves up to the minimum point, the shutdown energy can be obtained. Both curves give approximately the same results – 1120 J and 1130 J – which compare well with the latent heat energy stored in the fluid charge of 2.7 g of ethane (1228 J at 200 K). It appears, therefore, that the shutdown process is largely due to a simple evaporation/condensation process.

A parameter normally taken to indicate the shutdown time is the time at which the rate of increase of evaporator temperature reaches a minimum. Figure 9 clearly shows that this occurs at t = 3.5 min after the initiation of shutdown for the 2 K/min case and at t = 5.3 min for the 1 K/min case. This is to be expected, as the higher heat input to the condenser suggested by the 2 K/min case will produce a more rapid evaporation of fluid and, hence, a quicker shutdown. Figure 10 shows shutdown time plotted as a function of the rate of increase of condenser temperature. As would be anticipated, the curve becomes asymptotic at both ends of the scale, and accelerating the rate of increase of condenser temperature above 3 K/min does not substantially reduce the shutdown time.

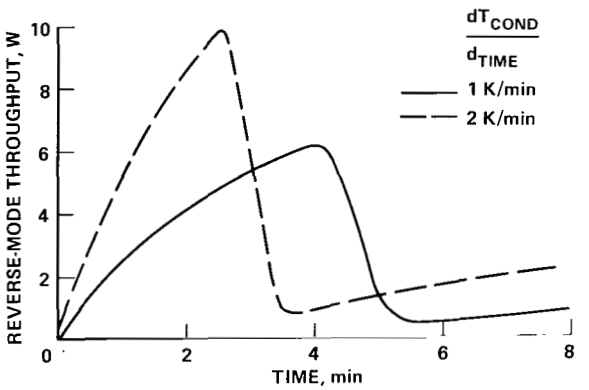

Figure 8.– Transient shutdown power curves (liquid trap).

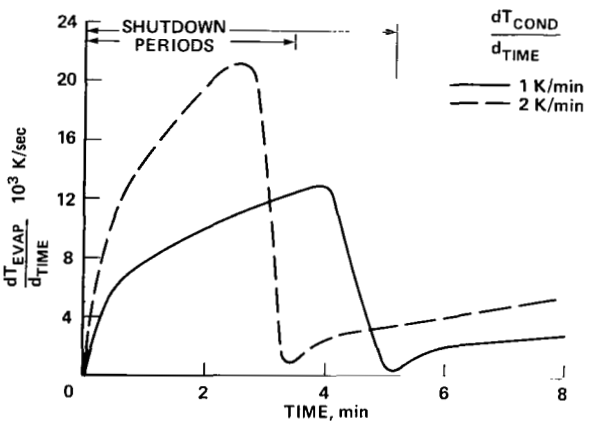

Figure 9.– Rate of increase of evaporator temperature vs time (liquid trap).

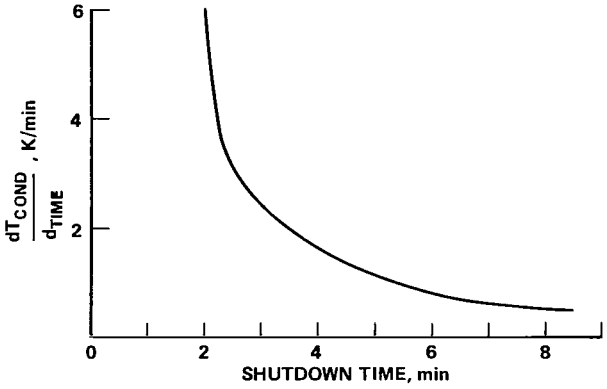

Figure 10.– Shutdown time as a function of rate of increase of condenser temperature.

The temperature time history of the condenser and evaporator for a full reversal and recovery to forward-mode operation is shown in figure 11. The inputs to the condenser block node for this situation were:

Nodal

Time, min	Temperature, K
0:00	180.0
20:00	200.0
40:00	180.0
50:00	180.0

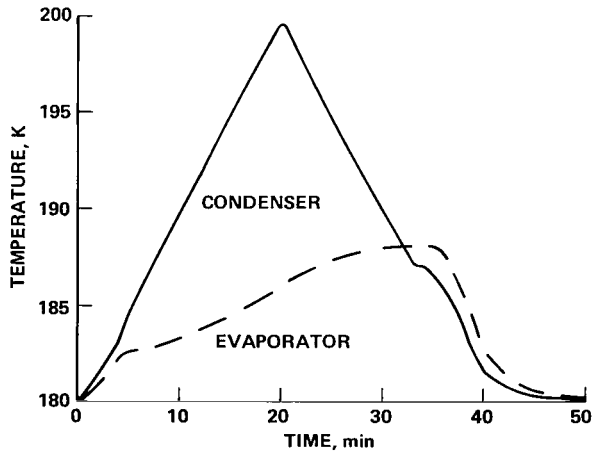

Figure 11.– Temperature profiles for reversal and recovery to forward-mode operation.

Linear interpolation was used to obtain the condenser block temperature between these points. The figure shows that the evaporator temperature follows the condenser temperature for the first 4–5 min after the initiation of shutdown. At this point the derivative of evaporator temperature with respect to time is a minimum (see fig. 9). The condenser temperature then breaks away with the heat transferred to the evaporator after this time being probably by conduction only. The upward-curving evaporator characteristic tends to level off after t = 20 min as a result of the decreasing temperature difference between the evaporator and condenser.

After t = 32 min, the condenser temperature drops below the temperature of the evaporator and trap and fluid starts to evaporate from the trap. There is a time delay of 2–3 min before the evaporator temperature can be brought under control, that is, the reversal of the temperature profile. This is because of the finite time taken to evaporate fluid from the trap and for the diode to resume forward-mode operation. The diode then continues to cool down to 180 K in a near isothermal condition while maintaining its forward-mode operation.

Figure 12 shows a comparison of the analysis of reference 5, which is based on a simplified three-node model. The analysis assumes that after the initiation of shutdown an adverse temperature gradient develops along the heat pipe. The respective heat flow by heat pipe action was designated $\dot{Q}_{hp} = C_f(T_{vond} - T_{evap})$. With increasing temperature gradient, $\dot{Q}_{hp}$ increases until the maximum heat transport capability of the heat pipe, $\dot{Q}_{max}$, is reached. As was already stated, $\dot{Q}_{max}$ is a function only of liquid inventory,

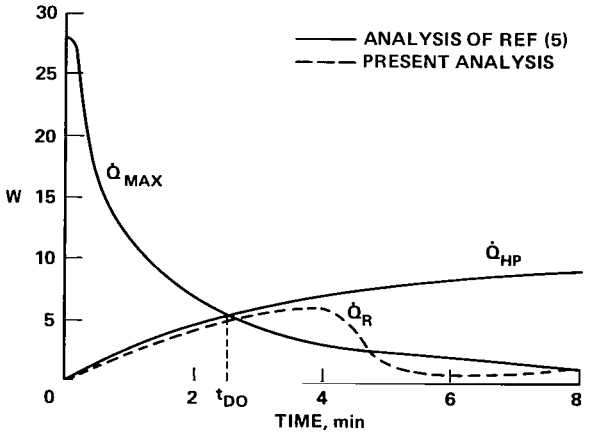

Figure 12.– Comparison of shutdown models.

M_L; as M_L decreases with time, $\mathring{Q}_{max}$ will also decrease as shown in figure 12. The intersection of these curves has been designated t_{DO}, the time at which the heat pipe begins to dry out. The shutdown period can thus be divided into two sections:

$$0 \leqslant t \leqslant t_{DO} \qquad \mathring{Q}_{SD} = \mathring{Q}_{hp}$$

$$t \geqslant t_{DO} \qquad \mathring{Q}_{SD} = \mathring{Q}_{max}$$

The area under this curve represents the total shutdown energy. In the present analysis, the sensible heat of the condenser and condenser block are taken into account, whereas in reference 5 they are neglected. Thus, in the present analysis, less heat is available for evaporation of the fluid from the condenser as a portion of the total heat input is used to raise the temperature of the condenser block. This results in longer dryout times as shown in figure 12 (2.5 min as opposed to 4 min); however, the shutdown energies are approximately the same.

A comparison of these predicted and observed behaviors is made in a later section.

Liquid-Blockage Diode

In a similar manner to the liquid-trap diode, a thermal nodal model was constructed for the liquid-blockage diode (fig. 13). As was the case for the liquid-trap diode, the analysis of the liquid-blockage diode assumes isothermal conditions at the onset of shutdown.

The transient response of the liquid-blockage diode is governed by the rate of evaporation of fluid from the reservoir and condenser. This vapor migrates to the evaporator, which is now the cold end, where it condenses and blocks off the part of the evaporator which it fills. Heat transfer to the evaporator walls is thus severely limited due to the low thermal conductivity of the liquid.

The inputs to the nodal model were ramp functions to the condenser and reservoir blocks (nodes 1 and 5). A portion of this heat input was taken up in raising the temperature of the condenser block and condenser, and the reservoir block and reservoir. The remainder was available to evaporate the fluid from the condenser and reservoir. The conductance between node 3 and node 6 was then adjusted in relationship to the length of evaporator section blocked by the condensing vapor, that is, the area term in the conductance from node 3 to node 6 ($G_{3-6} = hA_e$) was decreased as the blocking action progressed.

Figure 14 shows the energy transferred as latent heat to the evaporator during shutdown for a 1 K/min input to nodes 1 and 5. This constitutes only a portion of the latent heat available, as the amount of fluid required to block the vapor space in the evaporator is much less than the total amount of fluid available for blockage in this design. The vapor space volume in the evaporator is 1 cm^3; thus, a latent heat energy of 250 J (with ethane at 200 K) can be given up in this volume. The area under the curve in figure 14, 265 J, is in good agreement with this figure. As shutdown continues, additional fluid is condensed in the volume between the evaporator and the orifice plate. The resulting rate of increase of evaporator temperature as a function of time is shown in figure 15. In comparing this figure with the liquid-trap case (fig. 16) it can be seen that shutdown of the liquid-blockage heat pipe occurs first, 1.3 min before that of the liquid-trap diode. However, the

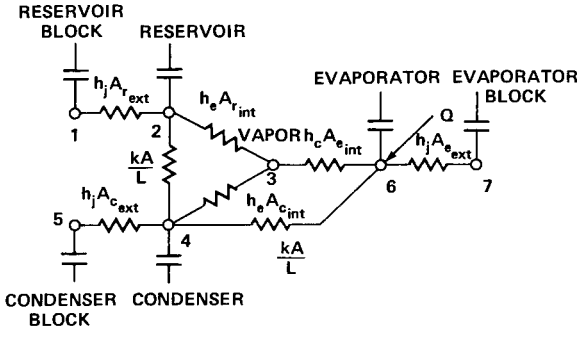

Figure 13.– Thermal nodal model for liquid-blockage diode.

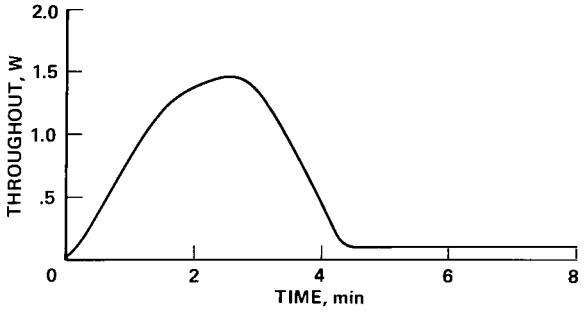

Figure 14.– Heat transfer to evaporator during shutdown.

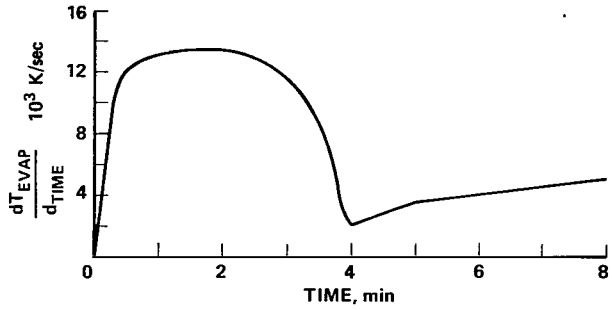

Figure 15.– Rate of increase of evaporator temperature vs time (liquid blockage).

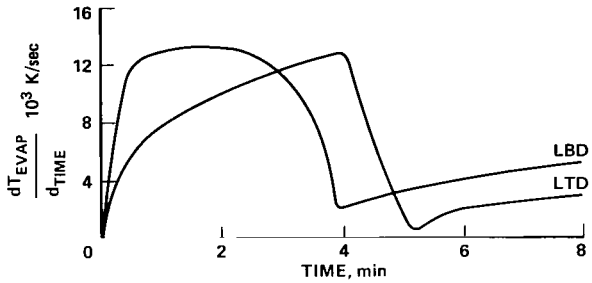

Figure 16.– Comparison of rates of increase of evaporator temperature vs time.

rate of increase of evaporator temperature of the liquid-blockage diode after shutdown is greater due to the larger reverse-mode conductance of the blockage diode (which includes a term for the thermal conductivity of the blocking liquid).

Figure 17 shows the evaporator and condenser temperatures for shutdown and recovery to forward-mode operation. The linearly interpolated inputs to the model in this case were as follows.

	Temperature, K	
Time, min	Node 1	Node 5
0:00	180.0	180.0
20:00	200.0	200.0
40:00	180.0	180.0
50:00	180.0	180.0

In a manner similar to that of the liquid-trap diode, the liquid-blockage evaporator follows the condenser temperature for the first 4 min after the initiation of shutdown. This is because of the adverse heat piping action and the finite time required to fill the

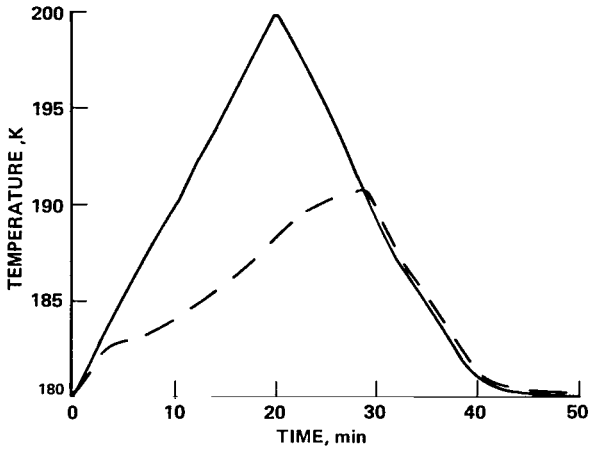

Figure 17.– Temperature profiles for reversal and recovery to forward-mode operation (liquid blockage).

evaporator vapor space with fluid. All the other factors mentioned in conjunction with the liquid trap, such as the inflection point in the evaporator curve at t = 20 min, are also evident. However the rise in evaporator temperature in this case is higher (10.6 K as opposed to 8.1 K for the liquid-trap diode) as a result of the aforementioned larger reverse-mode conductance. Another difference is that the delay between the time that the condenser temperature drops below the evaporator temperature and the time that the heat pipe resumes forward-mode operation is not as large as the liquid trap case; that is, recovery is very rapid. The reason for this is that the evaporator and part of the transport section wick are already full of liquid, and the evaporation of the excess liquid serves to carry heat directly to the condenser and promote a rapid resumption of forward-mode operations.

EXPERIMENTAL RESULTS

Steady-State Forward-Mode Performance

A series of tests was carried out on these diodes both individually and in a parallel test configuration. The initial tests in the parallel mode attempted to start up the heat pipes directly in the forward mode by adding 3 W to each evaporator, allowing the diodes to thermally stabilize, and then increasing the heat inputs in increments up to the burnout

condition. Burnout for these cases is defined as the condition with the evaporator temperatures being 10 K, or more, above the transport section temperatures. Using this method of startup, both heat pipes burned out at 9 W, the theoretical prediction in a horizontal mode being of the order of 25–28 W. These premature burnouts were probably due to the inability of the wicking systems to completely prime by capillary action alone.

A previous liquid-trap diode (ref. 6) successfully employed a Clapeyron priming technique to fill the wick and was able to transport in excess of 1250 W-cm (26.5 W) in a horizontal orientation with ethane as the working fluid at 200 K. Similar results (25 W, 1187 W-cm) have been obtained with the present liquid-blockage diode. Full performance curves for these diodes are shown in figure 18. However, due to severe damage to the liquid trap, a new diode was commissioned and built by the same manufacturer to identical specifications. Unfortunately, even with Clapeyron priming, this diode has never carried more than 12 W and the forward-mode tests were therefore limited to low power conditions.

The condenser sections of both diodes were captured in the same block, therefore nominally identical conditions were experienced. Figure 19 shows the transient response of the heat pipes to step changes in heat input. As can be seen at the 2-W level, the temperature drop across the diodes is about equal. Both diodes reacted quickly to a step change in heat input; however, as the heat input was increased, the temperature drop across the liquid-blockage diode became greater than that across the liquid trap because of the increased resistance of the orifice plate. This trend increased until, with primed diodes, the temperature difference across the liquid-blockage diode at 20 W was 7 K while across the liquid-trap diode it was only 3 K.

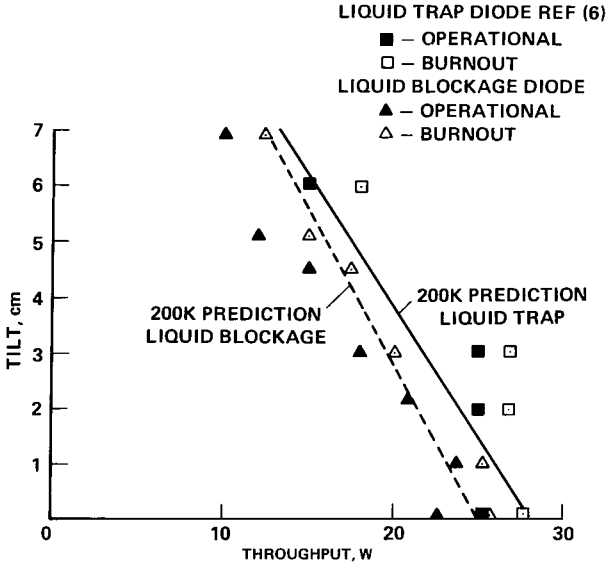

Figure 18.– Forward mode throughput characteristics.

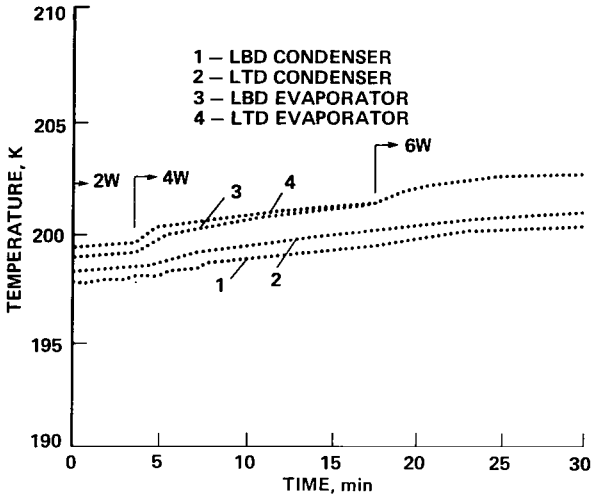

Figure 19.– Transient response to step change in heat input.

Reverse-Mode Performance

Reverse-mode and transient shutdown tests were conducted with the diodes in the parallel test configuration. In all cases the evaporator heater was left on during reversal to simulate a detector load.

Figures 20 and 21 show the diode temperature profiles during reversal. With 0.5 W of heater power to each evaporator and with the diodes operating in the forward mode, the liquid nitrogen supply was turned off and sufficient heat was applied to the condenser block to maintain a rise in temperature of approximately 1 K/min. Heat was also applied to the reservoir of the liquid-blockage diode to keep its temperature above that of the condenser, and to the trap to keep its temperature 1–2 K below that of the liquid-trap diodes evaporator. At t = 4 min the condenser temperature became greater than the liquid trap temperature, initiating shutdown for the liquid-trap diode; at t = 5 min the reservoir temperature became greater than the condenser and evaporator

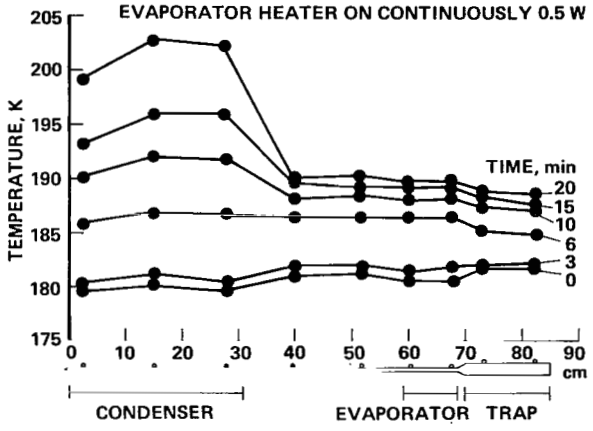

Figure 20.– Transient response of liquid-trap diode during shutdown.

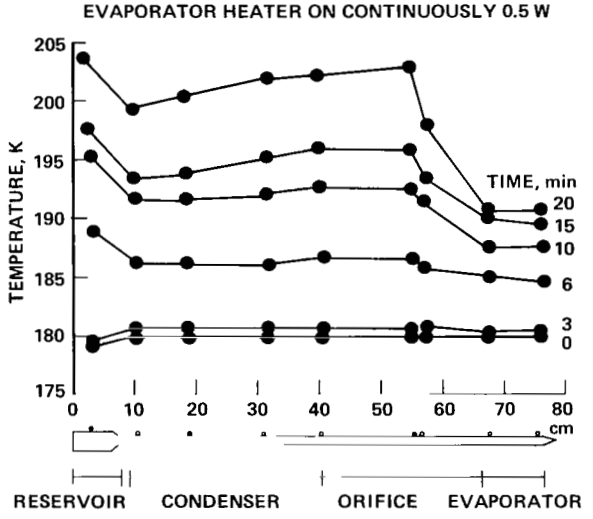

Figure 21.– Transient response of liquid-blockage diode during shutdown.

temperatures, hence commencing shutdown for the liquid-blockage diode.

After t = 10 min, clear evidence of shutdown can be seen in both pipes. Figures 22 and 23 show more clearly the transient temperature response of the condensers and evaporators. For the liquid-trap diode, t = 0 corresponds to the time when $T_{cond} > T_{trap}$ (4 min). Also shown in figure 22 is the theoretical evaporator temperature and the input to the thermal model in these cases being the actual condenser temperature histories. The figure shows that the thermal model predicts well the temperature excursion of the evaporator with theoretical shutdown occurring at t = 3.5 min and the experimental shutdown at $t = 3.5 \pm 0.5$ min.

For the liquid-blockage diode (fig. 23), t = 0 corresponds to the time at which $T_{res} > T_{evap}$ (5 min).

The thermal model again accurately predicts the transient evaporator temperature; however, in this case the shutdown occurs at $t = 2 \pm 0.5$ min whereas the theoretical model predicts 4 min.

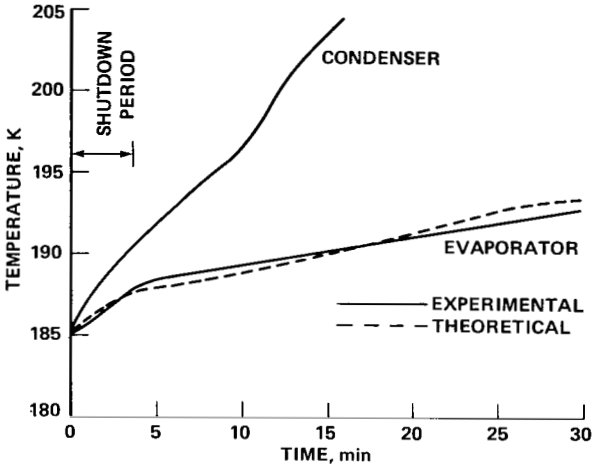

Figure 22.– Liquid-trap diode reverse-mode temperature profiles.

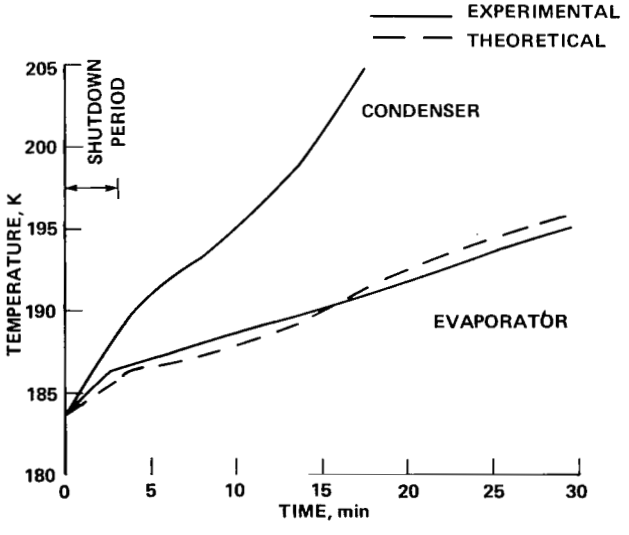

Figure 23.– Liquid-blockage diode reverse-mode temperature profiles.

The explanation for this is that while the theoretical thermal model is based on a pure evaporation process, the liquid removal from the reservoir is probably due to an expulsion process caused by vapor bubbles forming in the capillary channels of the reservoir (see appendix for a more detailed discussion). This process would result in a quicker depletion of fluid from the reservoir and hence produce a shorter shutdown time.

The energy absorbed by the evaporator or detector block during shutdown of the liquid-blockage diode can be obtained and is defined as:

$$Q_{SD} = MC_P(T_O - T_{SD}) - \dot{Q}_E t$$

where

MC_P = thermal capacitance of evaporator and detector block

T_O = temperature of block at initiation of shutdown

T_{SD} = temperature of block at complete shutdown

$\dot{Q}_E$ = evaporator power

t = shutdown time

Using this relationship, the shutdown energy was found to be 296 J, which compares well with the theoretical shutdown energy of figure 12 (265 J). The additional energy is probably due to radiation leakage from the vacuum chamber walls to the diode and radiation tunneling along the MLI. A conservative estimate for this heat leakage, using a simplified one-dimensional analysis, would be 3E-3 W/K which would account for an additional 37 J during the shutdown period.

In a similar manner, the shutdown energy can be obtained for the liquid-trap diode. However, due to the LN_2 cooling loop being in contact with the liquid trap, exact estimates of the shutdown energy cannot be obtained. Earlier individual tests performed without this cooling loop produced shutdown energies of 1150 J. This compares well with the results of the theoretical model in figure 8, 1130 J.

The reverse mode heat leakage for both diodes can be calculated and is equal to the time derivative of their respective evaporator temperature histories multiplied by their heat capacity:

	Liquid-trap diode	Liquid-blockage diode
Reverse-mode heat leak	0.406 W	0.66 W
Reverse-mode conductance (cond-evap)	.04 W/K	.07 W/K

Figure 24 shows a complete reversal and recovery to forward-mode operation for both the liquid-trap and liquid-blockage diodes operating in the parallel test configuration. The change in slope of the evaporator temperature profile of the liquid-blockage diode occurs at $t = 8 \pm 0.5$ min which indicates shutdown; this phenomenon does not occur until $t = 10 \pm 0.5$ min for the liquid-trap diode. However, the actual rise in temperature of the evaporator of the liquid-blockage diode is greater. The figure also shows that both heat pipe diodes return quickly to forward-mode operation as soon as the condenser drops below the evaporator temperature and the trap temperature becoming the hottest part, and reservoir the coldest part of their respective diode. However, this condition does not always occur. (See later section on Performance Limitations.) Both heat-pipe diodes after the reversal and recovery are able to transport 9 W but the liquid-trap diodes burned out at 12 W, indicative of a partially primed system. This behavior has been observed with all the liquid-trap diodes of this design that were

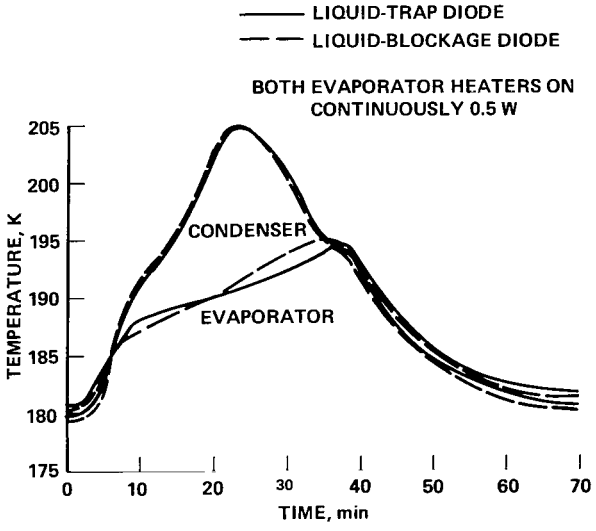

Figure 24.– Experimental temperature profiles for reversal and recovery.

tested, including the diodes which benefit from Clapeyron priming. After recovery, the liquid-blockage diode went on to transport 25 W before burnout.

Figure 25 shows a comparison of experimental reverse and recovery temperature profiles with the theoretical model for the liquid-trap diode. The controlled boundary node for the theoretical model was the condenser block node, which used the following inputs derived from the experimental results:

Time, min	Temperature, K
0.00	185.3
20:00	205.0
40:00	185.3
60:00	181.0

By controlling the condenser block node and allowing the condenser to find its own level, the steps which occur in the experimental and theoretical curves, after the crossover of the evaporator and condenser temperatures, can be compared. The figure shows that the step in the experimental curve occurs before, and is of a shorter duration than, the step in the theoretical curve. This is probably due to the aforementioned liquid expulsion from the capillary structure of the trap producing a more rapid recovery to forward-node operation (see appendix).

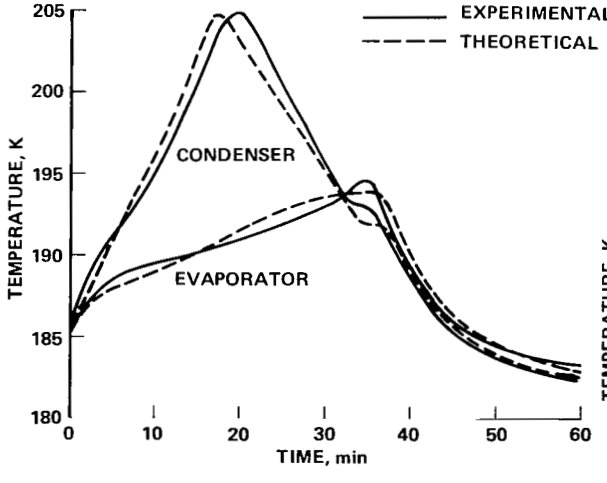

Figure 25.– Comparison of experimental reverse and recovery for liquid-trap diode with theoretical model.

Performance Limitations

There are several factors that can seriously affect the performance of both the liquid-trap and liquid-blockage systems. The repeated failure of these spiral artery diodes to start up in the forward mode has already been mentioned. Figure 26 shows another limitation where the liquid-trap diode has undergone a reversal and attempted recovery. This figure identifies two problems. For an evaporator power input of 1.5 W, an increase in evaporator temperature of about 24 K/hr can be expected. For the value of thermal capacitance represented by the size of evaporator block, the rate of temperature increase would probably not be satisfactory if a detector were being cooled; the maximum desirable temperature excursion probably is of the order of 10 K/hr. The other more serious factor evident from this test was that a condenser cool-down rate of 1.5 K/min was too fast for a recovery to forward-mode operation; that is, the temperature of the condenser keeps decreasing and evaporator temperature keeps increasing without displaying the coupling effect of heat pipe action. Rerunning this test with a cool-down rate of 1 K/min was successful in reestablishing forward-mode operation. The liquid-blockage diode was also susceptible to this phenomenon, although it did not occur until the cool-down rate was greater than 2 K/min.

Another important factor in the design of the diode system was the relative size and heat inputs of the condenser/reservoir configuration for the liquid-blockage diode and of the evaporator/trap configuration for the liquid-trap diode. With the

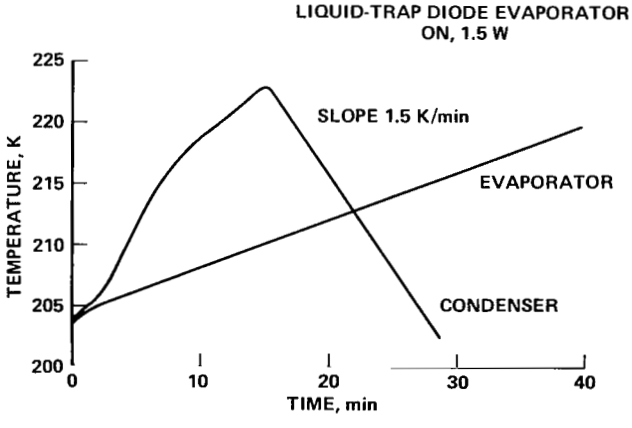

Figure 26.– Transient response during reversal and attempted recovery.

liquid-blockage diode, complete shutdown in a reasonable period of time required that the following criteria be established (ref. 4):

$$F_B = \frac{(Q/MC_p)\ res}{(Q/MC_p)\ cond} < 1 \qquad (2)$$

For an actual application, the heat inputs to the condenser and reservoir radiators would be, for example, from solar flux. The areas and respective thermal capacitances of the radiators would have to be adjusted to produce a rate of increase of reservoir temperature which was larger than that of the condenser. If these criteria are fulfilled, when the spacecraft goes into the shadow period the cool-down rate of the reservoir would be greater than that of the condenser. Figure 27 serves to show what happens under these conditions. For the first 20 min the shutdown of the diode continues as normal. However, at t = 21 min the reservoir temperature was allowed to drop below the condenser temperature. Almost immediately, the evaporator temperature started to rise, indicating that the fluid in the blocked portion must have migrated to the reservoir, thus opening the way for normal heat pipe operation to resume. This behavior was somewhat unexpected since at the time the reservoir temperature dropped below that of the condenser, the evaporator was still the coldest part of the diode, which was where the excess liquid should remain. This was not an isolated occurrence, the phenomenon being reproduced at a number of levels of tilt. The figure shows that the evaporator temperature rose by over 10 K in less than 3 min. The behavior of the heat pipe in this manner may be detrimental to the item being protected from thermal excursions by the diode. For actual applications therefore, F_B should be set approximately equal to 1.0; this will result in longer shutdown times but should alleviate the problems shown in figure 27. Thermally coupling the condenser and reservoir radiators should have the desired effect. In these experiments the relative condenser and reservoir block heaters have been adjusted so that F_B was slightly greater than 1.0 for the reversal and slightly less than 1.0 during the recovery to forward-mode operation.

A similar situation exists for the liquid-trap diode, the equation for this case being:

$$F_T = \frac{(Q/MC_p)_{trap}}{(Q/MC_p)_{evap}} < 1 \qquad (3)$$

This ratio ensures that the rate of increase of evaporator temperature is greater than the rate of increase of trap temperature during the shutdown process. If the reverse were true then shutdown would not occur because the trap temperature would be always greater than the evaporator temperature.

However, this inequality should not be too great. Figure 28 shows a reversal and recovery with

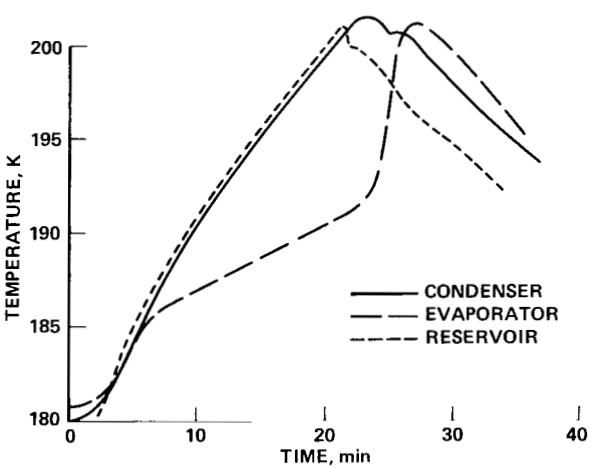

Figure 27.– Performance limitations for liquid-blockage diode.

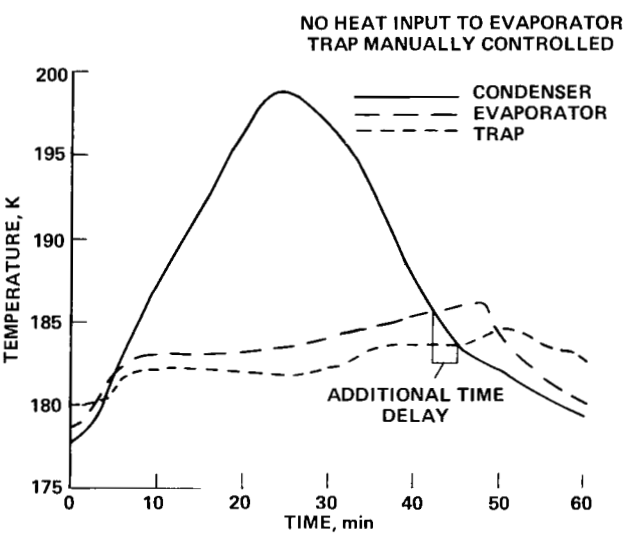

Figure 28.– Performance limitations for liquid-trap diode.

$3 > F_T > 1$. This results in a rapid shutdown with the trap temperature lagging the evaporator temperature. The penalty for this relatively large value of F_T is paid by virtue of a time delay after the condenser temperature drops below the evaporator temperature and the diode resumes forward-mode operation. The condenser temperature must in fact drop below the trap temperature before recovery to forward-mode operation can be initiated. In this case the delay is about 3 min and an additional 0.5 K rise in temperature for the evaporator with zero heat input. With the experiments discussed in the previous sections F_T was kept approximately equal to 1.0.

CONCLUSIONS AND GENERAL GUIDELINES FOR THE DESIGN OF A CRYOGENIC DIODE SYSTEM

1. Both liquid-trap and liquid-blockage diodes tested would not reliably start up in the forward mode, that is, start up after cool-down from ambient or restart after burnout. This feature is consistent with all diodes of this spiral-artery-wick design that were tested in this program. Limited success has been obtained with startup by employing a Clapeyron priming technique; the liquid-blockage diode appears to be more responsive to this primary process than the liquid-trap diode.

2. The liquid-trap and liquid-blockage diodes shutdown rapidly with any reversal of the normal temperature gradient, no auxiliary energy being required for this shutdown. The liquid-blockage diode achieves total shutdown from the forward mode faster than the liquid-trap diode (8 min as opposed to 10 min), with a smaller amount of energy transferred as latent heat to the evaporator (296 J as opposed to 1150 J). The liquid-blockage diode also has a smaller initial temperature rise of the evaporator for any given condenser profile. However, for longer shutdown periods (in this case greater than 20 min) the liquid-trap diode has the smaller evaporator temperature rise due to its lower reverse-mode conductance.

3. There is an upper limit for the cool-down rate of the condenser during recovery of the diodes to forward-mode operation, that is, the reinitiation of heat piping action cannot be guaranteed if this limit is exceeded. These cool-down figures were found to be approximately 1 K/min for the liquid-trap diode and 2 K/min for the liquid-blockage diode..

4. The relative size and heat inputs of the condenser/reservoir configuration for the liquid-blockage diode, and the evaporator/trap configuration for the liquid-trap diode are important factors in the operation of the diode system, that is, the values of F_B and F_T in equations (2) and (3) of the text. If F_B and F_T are set to be less than 1.0, shutdown cannot be initiated. Setting F_T and F_B to greater than 1.0 also has its difficulties. With the liquid-trap diode the penalty is relatively small, namely, a time delay before forward-mode operation can be resumed and is accompanied by a further increase in evaporator temperature. However, with the liquid-blockage diode the penalty is more severe. As soon as the reservoir temperature drops below the condenser temperature, the heat pipe appears to resume forward-mode operation resulting in a rapid increase of evaporator temperature (see fig. 27). This may be detrimental to the item being protected from thermal excursions of this sort by the diode. It is recommended therefore that F_B be set as close to 1.0 as is practically possible. This will result in longer shutdown times but will alleviate the problem described. Thermally coupling the condenser and reservoir should have the desired effect.

5. The liquid-trap diode would not recover to full forward-mode operation after reversal, transporting only 30% of its fully primed capacity. The liquid-blockage diode, on the other hand, transported heat up to its theoretical maximum (25 W). This may be due to the fact that the blockage diode's wick was partially full of fluid at the time of recovery, whereas the liquid-trap diode's wick was dry.

6. The detector or evaporator loads had to be kept below 1 W for this size of evaporator block (0.168 kg) so that the rise in evaporator temperature could be kept within reasonable bounds during reversal. For this situation therefore, where effective lengths are small, it appears unnecessary to use a high performance heat pipe such as this at only a fraction of its capacity.

7. The removal of liquid from the reservoir of the liquid-blockage diode during reversal and from the trap during recovery appears to be caused by an expulsion process rather than by direct evaporation. This promotes a more rapid shutdown in the case of the liquid-blockage diode and a more rapid recovery in the liquid-trap diode.

GENERAL OBSERVATIONS

The liquid-trap diode has a greater versatility in the choice of wicking system, almost any type of

wick being adaptable to this system. The liquid-blockage diode, however, is almost solely confined to an artery-type system.

The liquid-blockage technique is attractive for use in systems that have a short evaporator and a long condenser. In this system, the amount of fluid required for blockage can be minimized and thus a small reservoir can be used. This results in a weight saving over a liquid-trap diode whose reservoir must be sized to hold all the fluid in the pipe. In the diodes tested, the trap reservoir was 2.58 times heavier than the blockage reservoir. Because of the larger liquid trap, for different diodes having identical outside diameters and a given wick, the highest specific volume and therefore lowest pressure can be obtained with the liquid-trap technique. The liquid-blockage diode also has a larger fluid charge. This may be an important factor for cryogenic diodes that have to be stored under ambient temperature for long periods of time, for example, in a prelaunch situation. This situation may be overcome to some extent in the liquid-blockage diode by employing a two-diameter design. The smaller outside diameter would be maintained in the evaporator and in the portion of the transport section that is to be blocked, and a larger diameter would be used in the remainder of the pipe. Not only does this provide a larger specific volume, it also prevents any excess liquid priming across the vapor space in the condenser and blocking off large portions of the condenser (ref. 7). This does however cut down the liquid blockage diode's weight advantage over a one-diameter liquid-trap system.

The small vapor spaces required in the blockage diode to support the pressure head of the liquid slug restrict the heat pipe to smaller capacity applications than a similarly sized liquid-trap diode. The actual application may restrict the choice of diode; for example, it may not always be possible to situate the liquid trap adjacent to the evaporator, or the reservoir of the blockage diode adjacent to the condenser.

The total available shutdown energy of the liquid-blockage diode is greater than that of the liquid-trap diode due to the larger fluid change. However, in the design employed, only a fraction of this latent heat energy was transferred to the evaporator of the liquid-blockage diode because of the small amount of fluid required to block the evaporator.

Ames Research Center
National Aeronautics and Space Administration
Moffett Field, California 94035, Sept. 18, 1978

APPENDIX

LIQUID EXPULSION PHENOMENA

Both the liquid-trap and liquid-blockage diodes' reservoirs are constructed from aluminum channel as described in table 1. It is thought that during reversal of the liquid-blockage diode and recovery to forward-mode operation of the liquid-trap diode, a liquid expulsion process takes place in these reservoirs. To examine this phenomenon, a glass model was built for use with a room temperature fluid (fig. 29). The capillary tube was sized so that the surface tension and fluid dynamic effects would be the same for the room temperature fluid (acetone) as for ethane in the actual reservoir at 200 K.

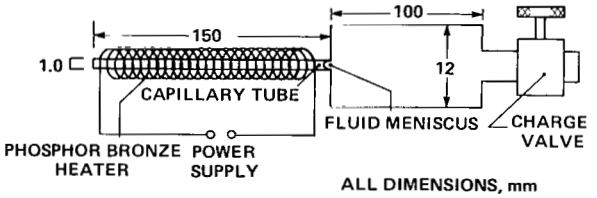

Figure 29.– Glass capillary model.

The capillary tube was filled with acetone and then operated in the reflux mode to expel any trapped air. Because of the very smooth glass walls of the capillary tube, bubbles could not be generated by heat input to the tube walls. However, vapor bubbles could be introduced into the capillary tube during the filling process. This procedure allowed tests to be undertaken to determine the time necessary to expel a given amount of fluid from the tube. The results indicate that when a vapor bubble is present, the liquid can be expelled from the tube in about 30% of the time required to empty the tube by evaporation alone. The calculations below give an estimate of the amount of superheat required to produce a vapor bubble in an actual reservoir situation.

Bubble Formation in a Diode Reservoir

If we consider a spherical vapor bubble of radius R in thermodynamic equilibrium with the liquid at pressure P_ℓ (fig. 30(a)) and, if σ is the surface tension

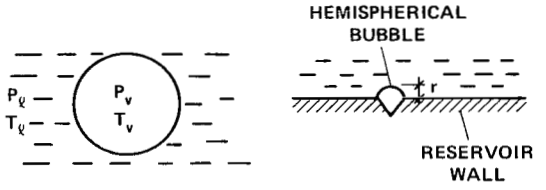

(a) Spherical vapor bubble. (b) Nucleation site.

Figure 30.– Bubble nucleation in diode reservoir.

and P_v the vapor pressure in the bubble, then a force balance gives

$$(P_v - P_\ell)\pi r^2 = 2\pi r\sigma \qquad \text{(A1)}$$

which gives

$$(P_v - P_\ell) = \frac{2\sigma}{r} \qquad \text{(A2)}$$

Equation (A2) suggests that for an infinitesimal bubble, the excess pressure required is infinite and bubbles cannot be produced. Thus, with pure gas-free liquids on very smooth surfaces it is possible to maintain high degrees of superheat. However, this is normally an unstable condition leading to explosive bulk boiling. In practice, dissolved gases and vapor trapped in surface roughness cavities can provide nucleation sites from which bubbles can grow with little superheat. The Clausius-Clapeyron equation provides a means by which this superheat can be determined:

$$\frac{dP}{dT} = \frac{h_{fg}}{T_{sat}V_{fg}} \simeq \frac{P_v - P_\ell}{T_v - T_{sat}} \qquad \text{(A3)}$$

where T_{sat} is the saturation temperature at P_ℓ.

Combining equations (A2) and (A3) we obtain

$$T_v - T_{sat} = \frac{2\sigma T_{sat} V_{fg}}{h_{fg} r} \qquad \text{(A4)}$$

If we assume that the diode reservoir walls have cavities of radius $r = 5\times10^{-4}$ cm (fig. 30(b)), the superheat required for bubble formation with ethane at 200 K from equation (A4) is $T_v - T_{sat} = 0.5$ K. Any superheat greater than this will enable the

bubble to grow in size, and eventually break away from the nucleation site when the bubble vapor pressure exceeds surface tension.

This simplified analysis together with observations of the glass model shows that very little superheat is required to promote bubble nucleation in the reservoirs. When these bubbles are present, the expulsion of liquid from the reservoirs due to bubbles expanding is a much faster mechanism than pure evaporation of fluid in the reservoirs.

REFERENCES

1. Kosson, R.; and Swerdling, B.: Design, Fabrication and Testing of a Thermal Diode. NASA CR-114526, 1972.
2. Quadrini, J.; and Kosson, R.: Design, Fabrication and Testing of a Cryogenic Thermal Diode. NASA CR-137616, 1974.
3. Brennan, P. J.; and Groll, M.: Application of Axial Grooves to Cryogenic Variable Conductance Heat Pipe Technology. International Heat Pipe Conference, Second. Bologna, Italy, 1976. Proceedings. Noordwijk, The Netherlands, European Space Agency, 1976, pp. 183–195.
4. Quadrini, J.; and McCreight, C. R.: Development of a Thermal Diode Heat Pipe for Cryogenic Applications. AIAA Paper 77-192, Jan. 1977.
5. Groll, M.; and Muenzel, W. D.: Design and Development of a Heat Pipe Diode. Phase I. Design. Institut für Kernenergetik Universität Stuttgart, Stuttgart Univ. (West Germany), Report No. ESTEC-2993/76/NL/PP/(SC), July 1977.
6. Williams, R. J.: Investigation of a Cryogenic Thermal Diode. AIAA Paper 78-417, May 1978.

1. Report No.	2. Government Accession No.	3. Recipient's Catalog No.
NASA TP-1369		

4. Title and Subtitle

TRANSIENT SHUTDOWN ANALYSIS OF LOW-TEMPERATURE THERMAL DIODES

5. Report Date
March 1979

6. Performing Organization Code

7. Author(s)

Richard J. Williams

8. Performing Organization Report No.
A-7642

10. Work Unit No.
506-16-31

9. Performing Organization Name and Address

NASA Ames Research Center
Moffett Field, Calif. 94035

11. Contract or Grant No.

13. Type of Report and Period Covered
Technical Paper

12. Sponsoring Agency Name and Address

National Aeronautics and Space Administration
Washington, D.C. 20546

14. Sponsoring Agency Code

15. Supplementary Notes

*NRC Resident Research Associate

16. Abstract

The various thermal diodes available for use in cryogenic systems are described. Two diode types, liquid-trap and liquid-blockage diodes, were considered to be the most attractive, and thermal models were constructed to predict their behavior in the reverse mode.

The diodes, which are of similar size and throughput, have also been examined experimentally in a parallel test setup under nominally identical conditions. Their characteristics are ascertained in terms of forward-mode and reverse-mode conductances, shutdown times and energies, and recovery to forward-mode operation with ethane as the working fluid in the temperature range 170 K to 220 K. Results show that the liquid-blockage diode is the quicker of the two diodes to shut down from the forward mode (8 min as opposed to 10 min). However, the liquid-blockage diode has a larger reverse-mode conductance which results in a greater overall evaporator temperature rise.

The importance of the relative size and heat inputs to the condenser/reservoir configuration of the liquid-blockage diode and the evaporator trap configuration for the liquid-trap diode are demonstrated.

Also included are data which show the susceptibility of the diodes to recovery to forward-mode operation. Guidelines for the choice of a particular diode for an actual application are given at the end of the report.

17. Key Words (Suggested by Author(s))	18. Distribution Statement
Cryogenic heat pipe Thermal diode	Unlimited STAR Category – 34

19. Security Classif. (of this report)	20. Security Classif. (of this page)	21. No. of Pages	22. Price*
Unclassified	Unclassified	20	$3.50

*For sale by the National Technical Information Service, Springfield, Virginia 22161

NASA-Langley, 1979

5 1 1U,D, 021779 S00903DS
DEPT OF THE AIR FORCE
AF WEAPONS LABORATORY
ATTN: TECHNICAL LIBRARY (SUL)
KIRTLAND AFB NM 87117